

# **STRESS DISTRIBUTION AND DETACHMENT MECHANISM PREDICTION OF ADHESIVE PILLARS**

A thesis submitted in partial fulfillment of the requirements for the award of the degree of

**Bachelor of Technology**

in

**Metallurgical Engineering**

Submitted by

**Varre Rohit**

**18MM01012**

Under the Supervision of

**Dr. Kisor Kumar Sahu**



**SCHOOL OF MINERALS METALLURGICAL AND MATERIALS  
ENGINEERING**

Indian Institute of Technology Bhubaneswar

**Bhubaneswar, Odisha, India**

**(May-2022)**

## **APPROVAL OF THE VIVA-VOCE BOARD**

**Date:** 13th May 2022

Certified that the thesis entitled “STRESS DISTRIBUTION AND DETACHMENT MECHANISM PREDICTION OF ADHESIVE PILLARS” submitted by “Varre Rohit”, Bachelor of technology student of the School of Minerals, Metallurgical and Materials Engineering, Indian Institute of Technology, Bhubaneswar for the award of Bachelors of Technology degree has been accepted by the internal and external examiner/examiners. The student has successfully defended his thesis in the viva-voice examination.

**Name of first Supervisor**

**(Supervisor)**

**Name of second Supervisor**

**(Supervisor)**

**Name of Examiner**

**(Internal Examiner)**

**Name of Examiner**

**(Internal Examiner)**

**Name of Examiner**

**(External Examiner)**

**Name of HoS**

**(Head of the School)**

## **CERTIFICATE**

This is to certify that the report entitled **“STRESS DISTRIBUTION AND DETACHMENT MECHANISM PREDICTION OF ADHESIVE PILLARS”**, submitted by **Mr. Varre Rohit (18MM01012)** to the Indian Institute of Technology Bhubaneswar, is a record of bonafide research under our supervision and the report is submitted for the end-semester evaluation of the Bachelor’s thesis work.

**Dr. Kisor Kumar Sahu**

**(Supervisor)**

## **DECLARATION**

I certify that

1. The work contained in the thesis is original and has been done by myself under the general supervision of my supervisor.
2. The work has not been submitted to any other Institute for any degree or diploma.
3. I have followed the guidelines provided by the Institute in writing the report.
4. I have conformed to the norms and guidelines given in the Ethical Code of Conduct of the Institute.
5. Wherever I have used materials (data, theoretical analysis, and text) from other sources, I have given due credit to them by citing them in the text of the thesis and giving their details in the references.
6. Whenever I have quoted written materials from other sources, I have put them under quotation marks and given due credit to the sources by citing them and giving required details in the references.

Varre Rohit  
18MM01012

## Abstract:

Over the past few decades, considerable effort has been expended to improve the adhesive characteristics of adhesive bi-phase pillars by optimizing the interfacial stress distribution. However, there are two major challenges to this approach.

1. The simulation of stress distributions takes a lot of computational power and time.
2. There is no reliable method to find out the detachment mechanism of the pillar without computing the stress distributions. Stable detachment can be obtained if the detachment is initiated from the center. After computing the stress distributions, corner detachments are discarded as their mechanism is unstable. Therefore, a lot of computational power is being wasted.

In this study, deep neural networks are used to predict the stress distribution of a bi-phase pillar from the 3rd order bezier curve control points which represent the interface curvature. 59292 data sets have been generated using COMSOL multiphysics software. Each data set consists of 1500 nodes across the 1mm radius(axis symmetry). The corresponding 1500 y coordinates of the curve are fed to the model to maintain a one-to-one relationship between labels and features. A robust scaler is used to filter out the outliers in the stress data set. A mean squared error of 0.55 is obtained by training the deep learning model.

Convolutional Neural Networks are used to predict the detachment mechanism from the curve images. The detachment mechanism is calculated by taking the difference in the integration of the stress distribution in the corners and at the center and stored in a variable Net.

$\text{Net} > 0$    Corner detachment

$\text{Net} < 0$    Center detachment

23017 data sets have exhibited center detachment and the model predicts the detachment mechanism with an accuracy of 96.2

# Contents

<b>Abstract</b>	<b>5</b>
<b>1. Introduction:</b>	<b>7</b>
1.1 Inspiration	7
1.2 Context of the study	9
1.3 Overview of the problem	11
1.4 Problem statement	11
<b>2. Literature review</b>	<b>12</b>
<b>3. Methods</b>	<b>16</b>
3.1 Simulation Protocol	16
3.2 Data Generation	19
3.3 Data Preprocessing	19
3.3.1 Stress Prediction	20
3.3.2 Detachment Prediction	20
3.2 Machine Learning Model	22
3.2.1 Stress Prediction	22
3.2.2 Detachment Prediction	24
<b>4. Results and Discussion</b>	<b>26</b>
4.1 Stress Prediction	26
4.2 Detachment Prediction	28
<b>5. References:</b>	<b>29</b>

# 1. Introduction:

## 1.1 Inspiration

Many insects can cling to flat substrates and walk on them, even if their claws can't help with mechanical interlocking. Ladybird beetles, for example, have adhesive pads made up of adhesive tarsal setae that allow them to connect to and walk on flat, smooth surfaces. The adhesive tarsal setae of ladybird beetles have a length of several tens of microns, and the leading edge has a component that helps to contact creation, adhesion, and friction with a size of several microns to 10  $\mu\text{m}$  and a lanceolate-like, pointed, spatula-like, or discoidal shape. The setae's Young's modulus varies along its length, ranging from 6.8 GPa at the base to 1.2 MPa at the tip<sup>6</sup>. The attachment is reversible, and rapid peeling saves energy during detachment.

The setae are protected by fluid secretion. The amount of secretion has a big impact on adhesion. A considerable volume of secretory fluid has been shown to considerably diminish adhesive strength. The secretory fluid has a different composition depending on the insect type. Lipids are the most important component in the ladybird beetle. The forces that contribute to adhesion are proportional to the liquid layer thickness. Understanding the principles of adhesion in biological systems requires knowledge of the properties of this secretory fluid and the thickness of the liquid layer in the contact area between the footpad and substrate. Due to surface tension, capillary forces dominate in a thicker layer, whereas the Laplace pressure takes over in a layer that is sufficiently thinner than the solid surface sandwiching the liquid. Intermolecular interactions with the substrate surface become conceivable when the fluid layer thickness is lowered further (less than 10 nm).

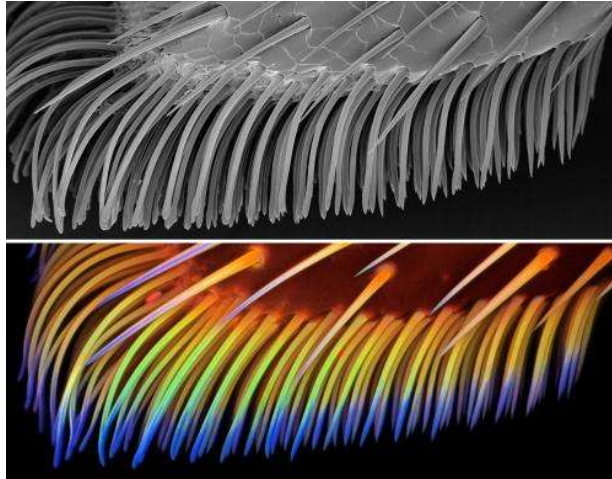


Figure 1.1: Stress distribution of setae in a Ladybug.

For years, scientists have been amazed by gecko feet, which let these lizards produce a compelling adhesive force. Microscopy has shown that a gecko's foot has nearly five hundred thousand keratinous hairs or setae. Each 30–130  $\mu\text{m}$  long seta is only one-tenth the diameter of a human hair and contains hundreds of projections terminating in 0.2–0.5  $\mu\text{m}$  spatula-shaped structures. Gecko setal arrays have the excellent ability of self-cleaning, which has a considerably wider potential application than pressure-sensitive adhesives (PSA) in several areas, such as robotics for rescue and detection, counter-terrorism, chemical sensing, and space positioning. A considerable number of studies have been devoted to understanding the interrelated frictional adhesion properties and mechanisms of gecko feet, hairs, and setae in order to mimic the gecko's swift movement on walls and ceilings.

Wall-climbing robots based on gecko-inspired adhesives have several advantages over those based on vacuum suction, magnetic adsorption, or velcros, such as small size, flexible and controllable articulation capability, self-cleaning property, and adaptability on rough surfaces. Therefore, research on the attachment and detachment mechanisms of gecko feet and hairs and the overall design of gecko-inspired adhesives are of great interest for both theoretical and practical applications on unique functional surfaces, articulated robots, and related devices.



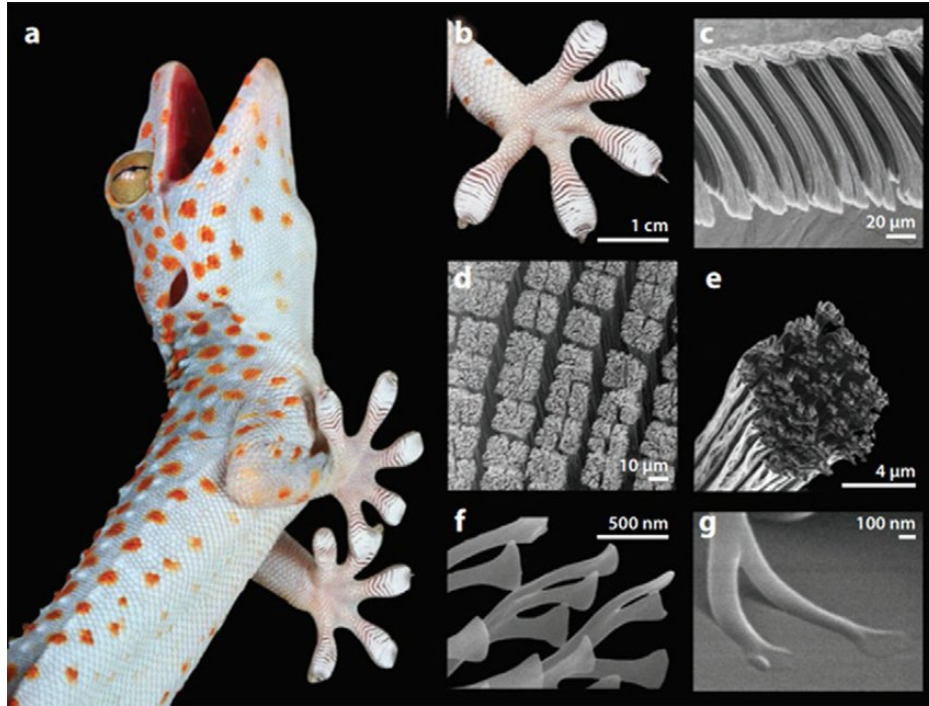


Figure 1.2: Structural Hierarchy of gecko adhesive system.

## 1.2 Context of the study

Even though the mechanisms of adhesion are different in geckos and ladybird beetles their fundamental mechanism is to alter the stress distribution for maximum adhesion. Various stress distribution analyses have been conducted on pillars to understand the adhesion properties with respect to the stress distributions.

Pillars are broadly classified into two types - mushroom fibril and flat punch. The flat punch pillar has a uniform radius throughout the length. It has stress singularities at the corner due to a sudden spike in the stress values at the edge of the pillar. On the other hand, the mushroom fibril pillar has a longer diameter at the base which results in a reduction of the average stress in the corners.

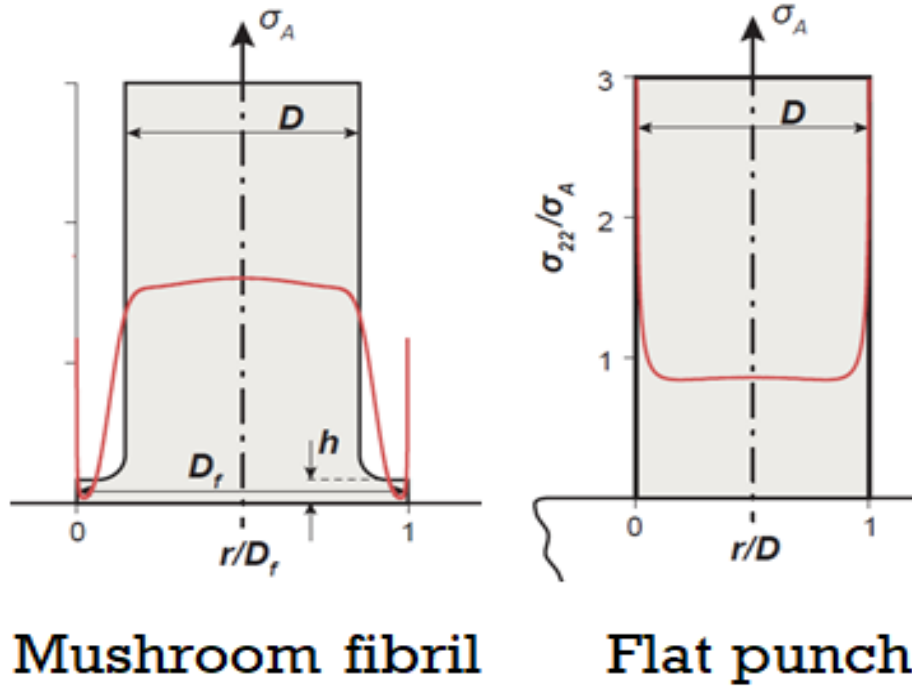


Figure 1.3: Stress distributions of mushroom fibril pillar and Flat punch pillar.

In order to achieve good adhesion, recent modeling studies have highlighted the need to optimize the distribution of interfacial stresses. Following biological examples, fibrils with a spatula and mushroom-shaped tips have been shown to have greater adhesion performance on numerous occasions. The key reason for enhanced adhesion, according to numerical simulations, is the lowering of stress magnitudes associated with the corner singularity, which is expected to operate as a fracture initiation point in the flat punch pillars.

The detachment of a single flat punch pillar takes place as a consequence of the destabilization of an interfacial void whose size increases following a crack-like propagation process. The detachment can initiate either at the corner or at the center of the pillar. Studies have shown that, when center crack propagation dominates, based on the crack size and on the tip thickness, the detachment mechanism is stable. Center crack stability finally provides the theoretical limit on the detachment strength of the adhesive.

## 1.3 Overview of the problem

To optimize the stress distribution, simulation softwares like COMSOL multiphysics can be used along with optimization algorithms. But, the major challenges to this approach are:

1. For high precision, dense meshes are needed for the simulation which would need a very high computational power. To optimize the distribution, large datasets are required with high precision which would need an enormous amount of computational time.
2. The detachment mechanism is stable when the detachment occurs at the center. There is no method to specify if the detachment takes place at the center or at the corner without performing the simulation. Even though the corner detachment is not the field of interest, they have to be simulated to determine the detachment mechanism and later omitted from the optimization as they are corner detached. This wastes a lot of computational power and time.

## 1.4 Problem statement

This project focuses on using deep learning techniques to reduce the computational time required to perform the simulations and optimize the stress distributions. The problem statement can be divided into two parts:

1. Design a deep neural network to predict the stress distribution of a bi-phase pillar from the curve coordinates of the interface. A large number of samples can be generated with the deep learn model which requires a fraction of the computational time taken by the simulation software.
2. Determine the detachment mechanism of the bi-phase pillar by using deep learning models directly from the bezier control points. This leads to the elimination of the need to perform simulations to predict the detachment method.

## 2. Literature review

### 1. Designing adhesive pillar shape with deep learning-based optimization

The shape optimizations in the previous studies are conducted by considering specific pillar forms with a few parameters, hence with limited design space. In this study, they presented a framework to find a free-form optimized adhesive pillar shape out of extensive design space. They generate 200 000 different shapes of mushroom-shaped adhesive pillars based on the Bezier curve with a few control points by considering two distinct edge shapes, sharp and truncated edges, to account for the limitation in the realistic manufacturing resolution. Deep neural networks are trained from the numerical simulations of the resulting interfacial stress distributions. For the training set, 1<sup>st</sup>-10<sup>th</sup> order Bezier curves were used to generate pillar shapes. 100,000 shapes each were generated for a sharp edge and truncated edge. An upward pull-off force with uniformly distributed normal stress  $\sigma_0$  is applied at the top of the pillar, and the interfacial stress distribution  $\sigma_{yy}$  at the bottom interface is calculated.

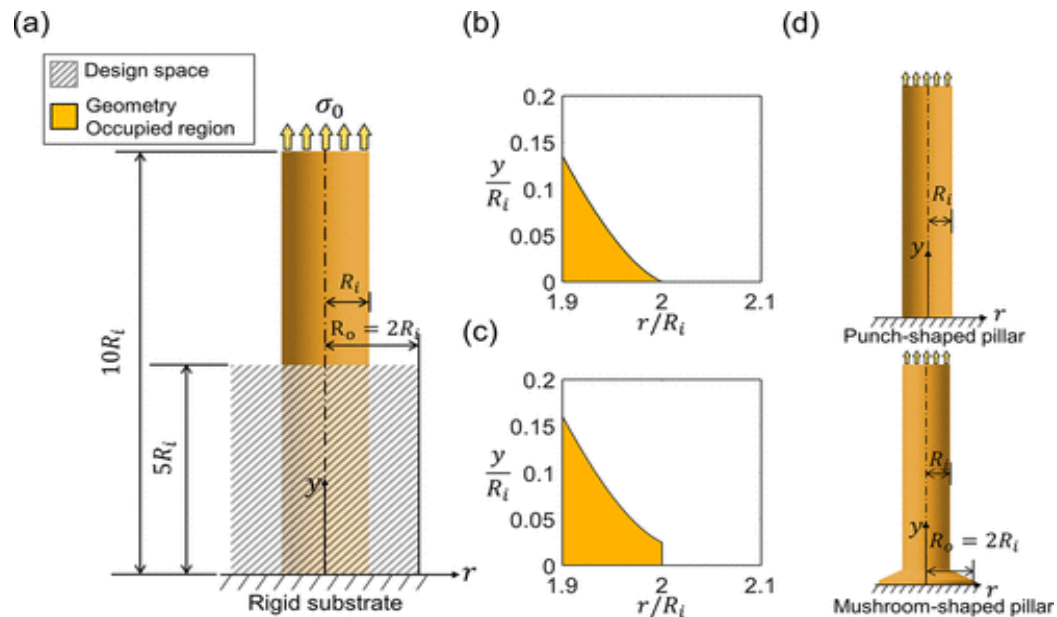


Figure 2.1: (a) Axial symmetric simulation model. (b) an ideally sharp edge and (c) a truncated edge (d) The punch shaped pillar and mushroom-shaped pillar

## 2. Composite Pillars with a Tunable Interface for Adhesion to Rough Substrates

Previous research has established the advantages of synthetic fibrillar dry adhesives for the temporary and reversible adhesion of hard objects with smooth surfaces. Surface roughness, on the other hand, results in a significant reduction in pull-off tensions, necessitating the need for updated design approaches. The cylindrical two-phase single pillars, which are comprised of a mechanically rigid stalk and a soft tip layer, are designed to achieve this goal. The adhesion of pillar structures to smooth and rough substrates is demonstrated to be greater than that of traditional pillar structures. The thickness of the soft tip layer, the ratio of Young's moduli, and the curvature of the interface between the two phases can all be adjusted to achieve the desired adhesion qualities. It was possible to get adhesion levels that were comparable to those obtained on smooth substrates when using rough substrates. With the concept of the composite pillar, it is possible to transcend the current practical restrictions imposed by surface roughness and open up new domains of application where roughness is ubiquitous.

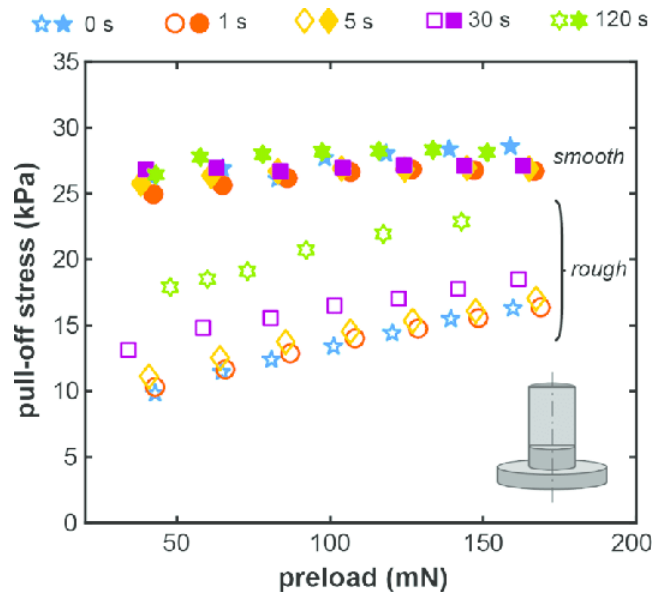


Figure 2.2: Pull-off stress of conventional pillars (controls) made entirely from polyurethane

### **3. Theoretical limits in detachment strength for axisymmetric bi-material adhesives**

When it comes to dry adhesives, short-ranged intermolecular connections are used, which means that they have a low elastic modulus and hence may conform to the surface roughness of the glued substance. Soft adhesives, on the other hand, store strain energy under external loads, which when released cause the development of interfacial defects, which ultimately results in detachment. The optimal adhesive is gentle but firm in this case. Using a bi-material adhesive with a soft tip for surface conformation and a firm backing for reduced strain energy release and hence improved adhesive strength, the solution to this contentious demand is found. This design strategy can be found in abundance in nature across a wide range of species.

Although the detachment mechanisms of these adhesives are poorly known, quantitative analysis of their adhesive strength has not yet been performed. We investigate the strength of axisymmetric bi-material adhesives using linear elastic fracture mechanics as a foundation. We found two main detachment processes, namely, (i) crack propagation and (ii) edge crack propagation, both of which were seen. If the soft tip is sufficiently thin, the mechanism takes over and allows for stable crack propagation, resulting in the toughening of the interface between the two materials. Finally, it is demonstrated that these adhesives have the highest theoretical strength possible by generating closed-form estimations for the detachment stress that are independent of the crack size, so making the interface defect tolerant.

#### **4. Numerical study of adhesion enhancement by composite fibrils with soft tip layers**

Bio-inspired fibrillar surfaces with reversible adhesion to stiff substrates have been thoroughly investigated over the last decade. This paper proposes a novel composite fibril consisting of a soft tip layer and stiffer stalk with differently shaped interfaces (flat vs. curved) between them. Tensile stress is applied remotely on the free end of the fibril whose other end adheres to a rigid substrate. The stress distributions and the resulting adhesion of such structures were numerically investigated under plane strain(2D) and axisymmetric (3D) conditions. The stress intensities were evaluated for different combinations of layer thickness and Young's moduli. The adhesion strength values were found to increase for thinner layers and a larger modulus ratio. The results of this paper provide a new strategy for optimizing the adhesion strength of fibrillar surfaces.

## 3. Methods

### 3.1 Simulation Protocol

From the literature review, it can be concluded that the stress distribution depends upon:

1. Elastic Modulus
2. Poisson's number
3. Density
4. Thickness and interface curvature

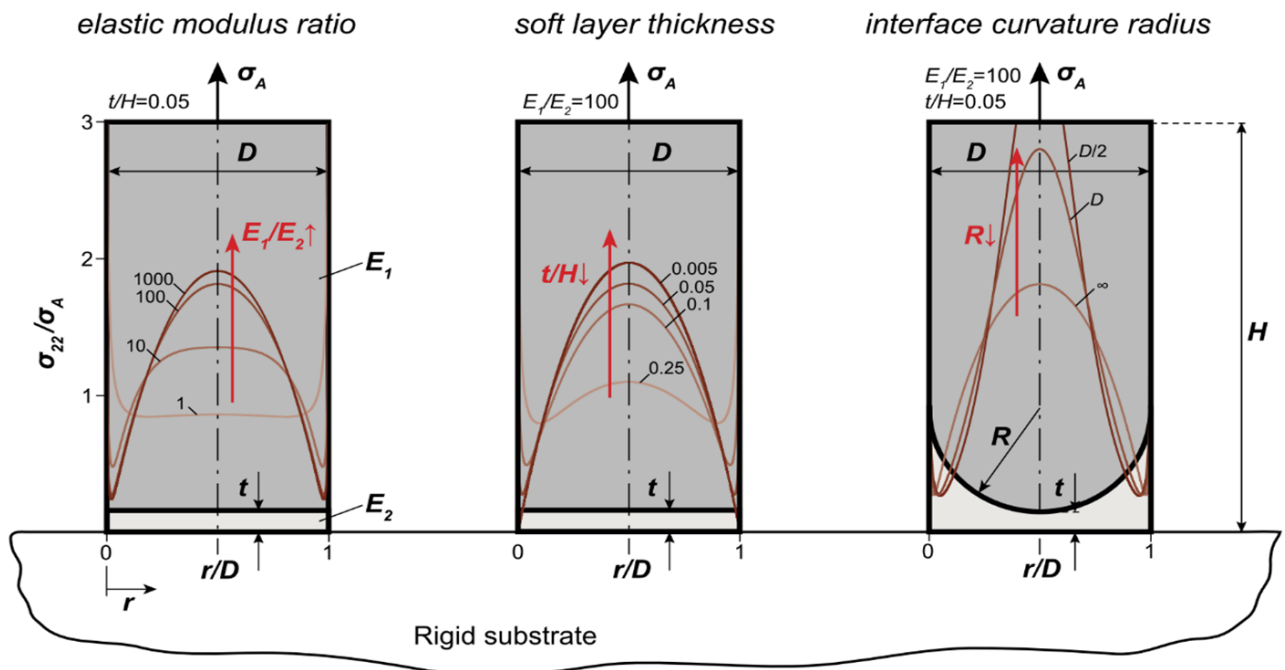


Figure 3.1: Stress dependency on (a) Elastic Modulus (b) Thickness and (c) Curvature

PDMS - Polydimethylsiloxane (PDMS) is one of the most widely used materials for the fabrication of gecko-inspired adhesives. PDMS has a Poisson ratio close to 0.5 and a density of 965kg/m<sup>3</sup>.



Upon reviewing research papers, the following parameters have been used for the simulation.

1.  $E=2\text{MPa}$
2. Poisson's number = 0.49
3. Density of  $965\text{ kg/m}^3$  (this is similar to Polydimethylsiloxane).
4. Define a 2 D geometry for the pillar of dimension 2 mm diameter and 4 mm height in contact with a rigid substrate.

Boundary conditions:

1. Symmetry axis
2. Boundary condition: fixed constraint which is the contact with the substrate
3. Apply a small displacement to the top of the pillar -  $100\text{ }\mu\text{m}$

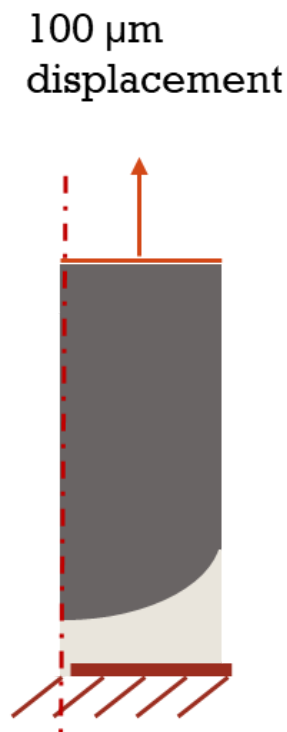


Figure 3.2: Sample simulation model representing the boundary conditions.

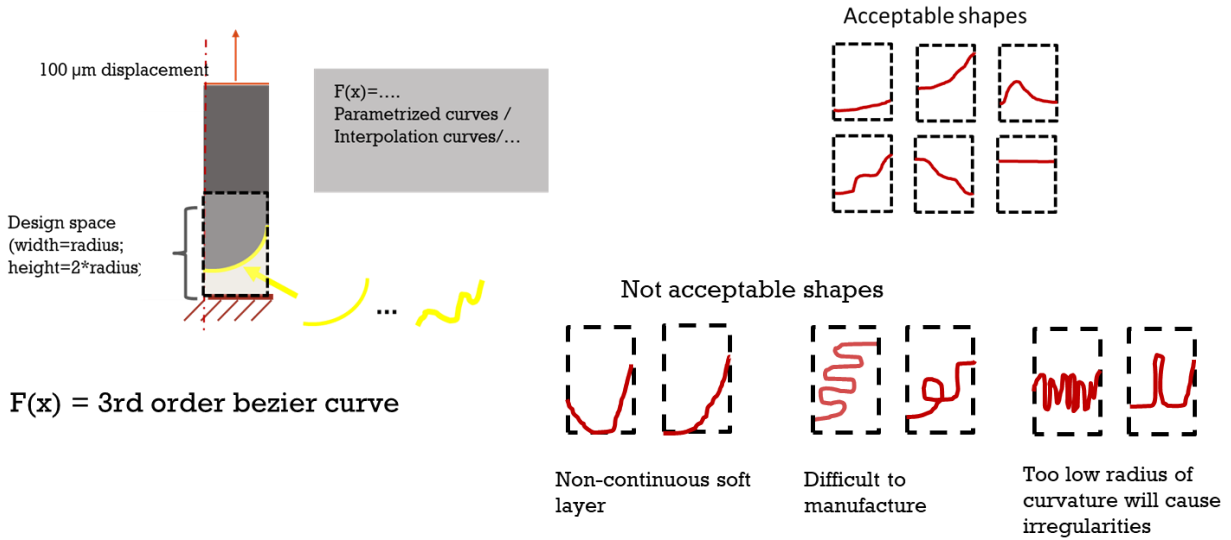


Figure 3.3: Interface protocol

The interface curves must satisfy the following:

1. It should be continuous.
2. It should be differentiable.
3. The curve should always be within the design space.
4. The radius of curvature should not be very high or very low.
5. The curve should never intersect each other.
6. There should be a unique y-coordinate for every possible x-coordinate.

To meet all these requirements, 3rd order Bezier curves are used to generate the interface. The random function is used to generate random control points with the constraint that the curve should always lie in the design box.

## 3.2 Data Generation

- COMSOL multiphysics software is used to simulate the stress distribution.
- MATLAB is connected to COMSOL via Livelink to automate the simulation.
- The base of the pillar is meshed into 1500 nodes to determine the stress distribution.
- The data is stored as a .csv file as 1500 ordered pairs(x,y) millimeters and pascal as the units respectively.
- 59262 data samples have been simulated.

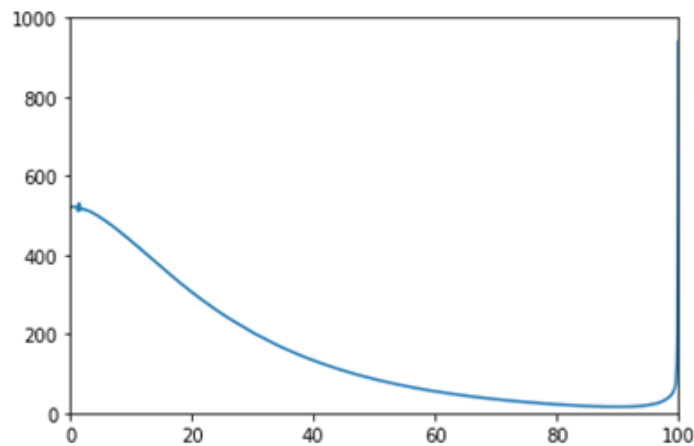


Figure 3.4: Sample stress distribution. Y-axis represents stress in  $10^{-4}$  pascal, and the x-axis represents the distance from the center of the cylinder in  $10^{-2}$  mm

## 3.3 Data Preprocessing

Pre-processing refers to the transformations applied to our data before feeding it to the algorithm. Data Preprocessing is a technique that is used to convert the raw data into a clean data set. In other words, whenever the data is gathered from different sources it is collected in raw format which is not feasible for the analysis.

### 3.3.1 Stress Prediction

For the stress prediction, the features are the y-coordinates of the curve for the corresponding node coordinates. From the bezier curves, the y coordinates are calculated from the control points by using the shapely library in python. Since there are 1500 nodes, 1500 y-axis coordinates are obtained as features.

The stress distribution values at 1500 node points are labels. There is a one-to-one relationship between the values and the labels as the y-coordinate of the curve corresponds to the respective stress value. This one-to-one relationship between the features and the labels makes it easier to optimize the machine learning algorithms.

### 3.3.2 Detachment Prediction

The detachment takes place at the location of higher stress. If the center of the pillar experiences higher stress, it would initiate detachment. Similarly, if the corner experiences higher stress, it would initiate detachment. The stress at the corner and at the center are calculated by summation of the stress distributions till the midpoint.

$$L = \sum_{i=1}^{750} \sigma \quad (\text{Stress at the center})$$
$$R = \sum_{i=750}^{1500} \sigma \quad (\text{Stress at the corner})$$
$$\text{Net} = R - L$$

If  $\text{Net} > 0$ , it means corner detachment is favoured. Similarly, if  $\text{Net} < 0$ , it means center detachment is favoured. To predict the detachment mechanism we would employ logistic regression which would take categorical outputs. Therefore, the corner detachment is labeled as 0 whereas the center detachment is labelled 1. Curves generated from the bezier control points are taken as features.

Since we are employing a 3rd order Bezier curve, four control points are necessary to define the curve which makes 8 coordinates. Using the Matplotlib library, the curve is plotted and stored as an image. Since the curve is already constrained in a bounding box, all the curves are already scaled. There is no need for scaling or standardization of the curves. X-coordinate ranges from 0 to 1 whereas y-coordinate ranges from 0 to 2. The curve is changed into greyscale from RGB to reduce the dimensions as color is not the point of interest.

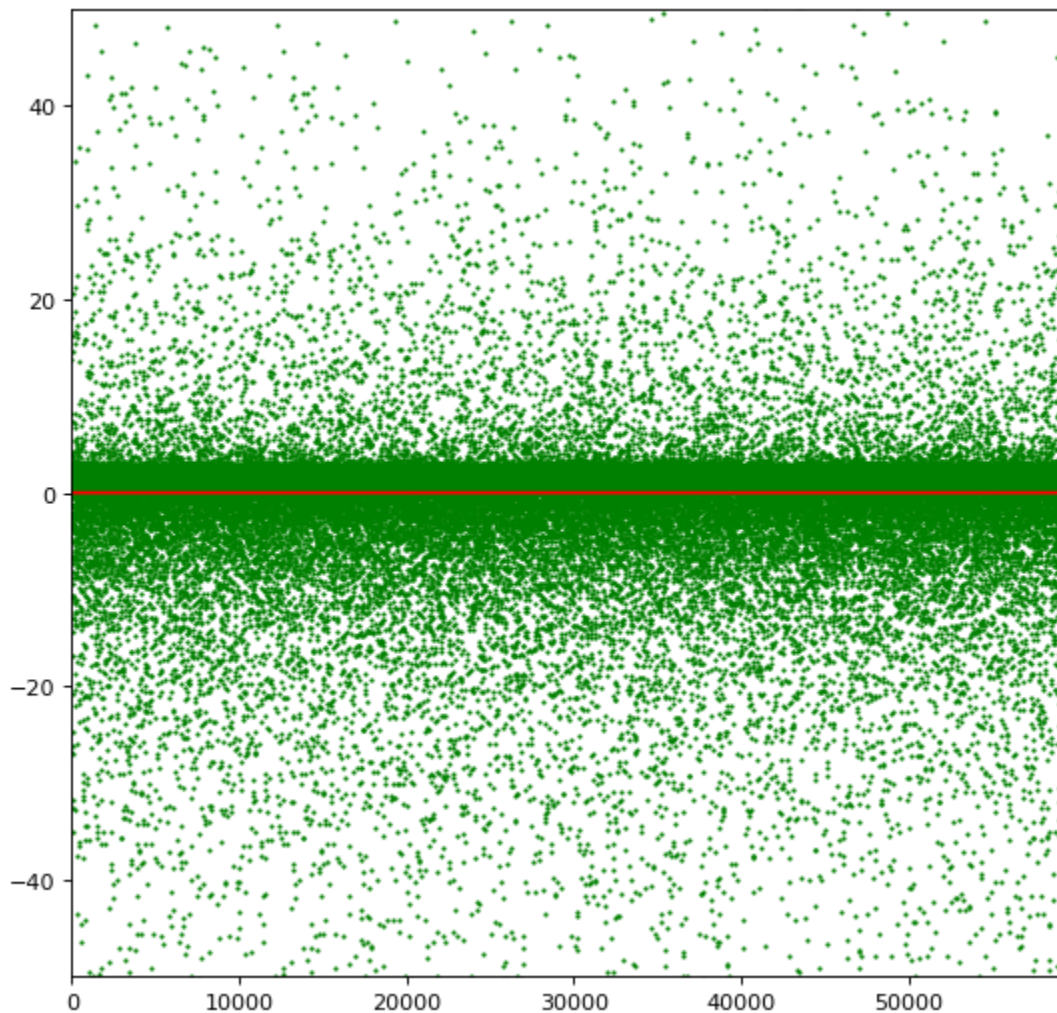


Figure 3.5: Net vs Frequency plot. The red line represents  $y = 0$  line.

Out of the 59262 data sets generated, 23017 have Net less than 0. This means 23017 out of 59262 favors center detachment. However, a majority of the data falls close to the  $y = 0$  line.

## 3.2 Machine Learning Model

### 3.2.1 Stress Prediction

The stress distributions which are to be predicted are susceptible to outliers. Training a deep learning model with outliers would make it very difficult for the model to learn. It is very important to get rid of the outliers to build the model efficiently. Moreover, data preprocessing aids the gradient descent and helps train the model quickly. When our data is comprised of attributes with varying scales, many machine learning algorithms can benefit from rescaling the attributes to all have the same scale. This is useful for optimization algorithms used in the core of machine learning algorithms like gradient descent. RobustScaler is used to remove the outliers and scale the dataset.

It scales features using statistics that are robust to outliers. This method removes the median and scales the data in the range between the 1st quartile and 3rd quartile. i.e., in between the 25th quantile and 75th quantile range. This range is also called an Interquartile range.

The median and the interquartile range are then stored so that they could be used in future data using the transform method. If outliers are present in the dataset, then the median and the interquartile range provide better results and outperform the sample mean and variance.

RobustScaler uses the interquartile range so that it is robust to outliers.

$$X_{\text{scale}} = \frac{x_i - x_{\text{med}}}{x_{75} - x_{25}}$$

1. RobustScaler is used from the sci-kit learn library to rescale the data. After applying the scaler to the stress distributions their values ranged from -0.5990909029673785 to 58.36777768718635. On the other hand, the stress values before preprocessing ranged from 51717.86062495772 to 42935207.31619579.
2. The data is divided by a train test split of 0.2 and a validation split of 0.2 by using the sci-kit learn library. 47433 data points are used for training the deep neural network.

3. Stochastic Gradient Descent with a learning rate of 0.02 and momentum of 0.9 is the model optimizer.
4. The model is trained for 30 epochs with a batch size of 128.
5. Mean squared error is chosen as the loss function.

$$\text{MSE} = \frac{1}{n} \sum_{i=1}^n (y_i - \tilde{y}_i)^2$$

6. The summary of the model is as follows:

Layer (type)	Output Shape	Param #
dense (Dense)	(None, 1500)	2251500
dropout (Dropout)	(None, 1500)	0
dense_1 (Dense)	(None, 1500)	2251500
dropout_1 (Dropout)	(None, 1500)	0
dense_2 (Dense)	(None, 2000)	3002000
dense_3 (Dense)	(None, 2000)	4002000
dense_4 (Dense)	(None, 2500)	5002500
dropout_2 (Dropout)	(None, 2500)	0
dense_5 (Dense)	(None, 1500)	3751500
dense_6 (Dense)	(None, 1500)	2251500
dense_7 (Dense)	(None, 1500)	2251500
Total params: 24,764,000		

### 3.2.2 Detachment Prediction

The detachment mechanism depends on various factors like - the slope of the interface, the curvature of the interface, etc. An artificial neural network with the coordinates as input cannot capture a significant amount of the insights from the continuous data which makes it inefficient to predict detachment. Therefore, convolutional neural networks are used, which are efficient to extract data (capture continuity) from images.

1. The datasets which have their  $Net < 0$  are labeled as 1 and those which have  $Net > 0$  as 0. The label set is obtained by converting this binary to one hot coding using the `to_categorical` function from `keras, utils`.
2. Scalers were not used as the data is already scaled according to the requirements of the bezier curve. The control points are in such a way that the curve is bounded in the design space.
3. Convolutional Neural Networks (CNN) are used to extract information from the greyscale curve images.
4. The data is divided by a train test split of 0.2 and a validation split of 0.2 by using the `sci-kit learn` library. 47433 data points are used for training the deep neural network.
5. Adams optimizer with a learning rate of 0.01 is the model optimizer.
6. The model is trained for 100 epochs with a batch size of 128.
7. Categorical cross-entropy and accuracy are chosen as loss function and metric respectively.



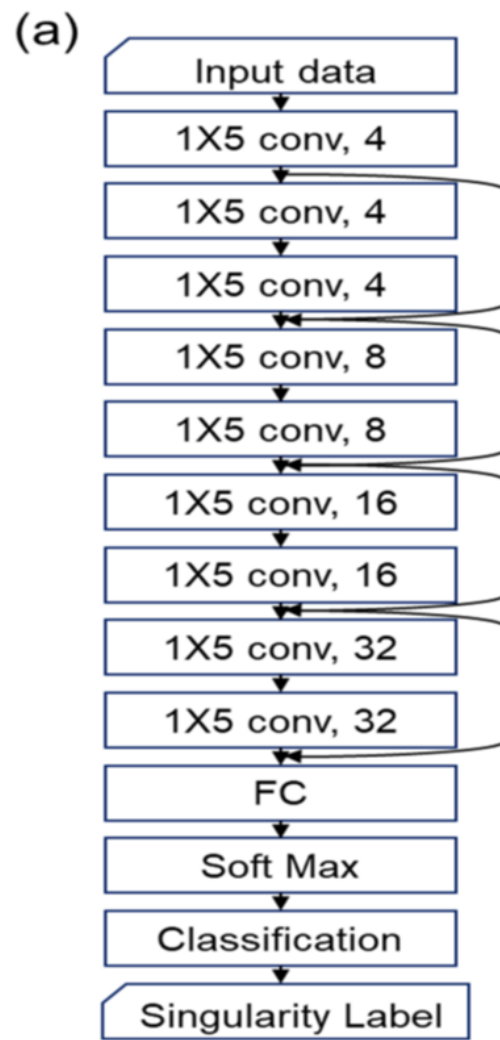


Figure 3.6: Neural network architecture

## 4. Results and Discussion

### 4.1 Stress Prediction

After training multiple models multiple times and fine-tuning the hyperparameters, the following results were obtained.

1. The predicted output is scaled as we have used a robust scaler before feeding the data into the model. Therefore, to generate the curves from prediction, the `inverse_transform` function of that robust scaler is used.
2. In the 1<sup>st</sup> epoch, the training loss and validation losses are approximately 78 and 91 respectively. By the end of the 20<sup>th</sup> epoch the loss is saturated to approximately - 0.658 in training and 0.673 in validation sets.
3. Steady gradient descent can be observed in Figure 4.1. During saturation, the validation and training loss have approximately the same loss. This means that the model is not overfitted.
4. By the end of the training, the loss function is as low as 0.53. This indicates a good model accuracy.
5. The test set got a loss of 0.55 which is very close to the training loss and validation loss. Thus, the model is well fitted and does not suffer from overfitting and underfitting problems.

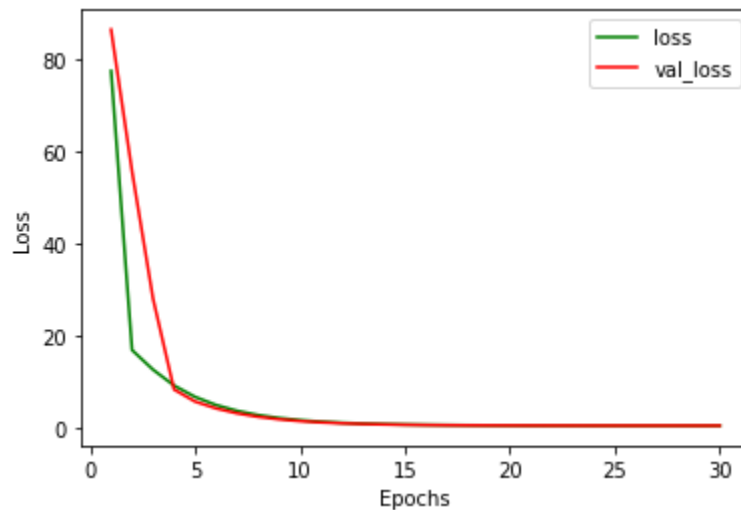


Figure 4.1: Loss vs Epochs of the deep neural network for stress prediction.

6. The actual stress distribution and predicted stress distributions are plotted. From Figure 4.2, it can be observed that there is a slight deviation in the predicted value from the actual value.
7. Even though the test loss is very low, there is a considerable amount of deviation, especially in the center of the pillar.
8. This might be due to the unique exponential behavior of the stress distribution. This makes the prediction to get biased toward the singularity because the loss component of the singularity is higher than the remaining part due to a very high singularity value.
9. Robust scalers, min-max, and standard scalers are generalized scalers which are usually used for uniform data distributions, customized data preprocessing techniques can be explored to better fit the curve.
10. Another approach is by dividing the stress distribution into two parts, singularity, and non-singularity. Two deep learning models were trained to predict the two curves, but the point at which these two curves have to be separated was a problem. The singularity starts in different curves at different coordinates, making it impossible to generalize the protocol of the separation of the two curves. Therefore this approach was discarded.

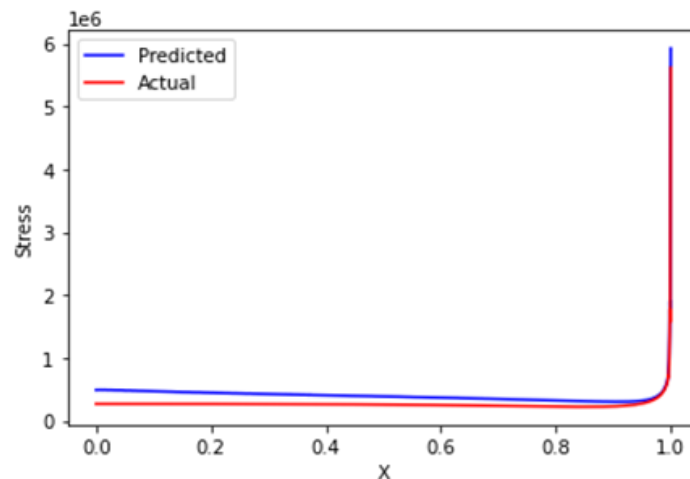


Figure 4.2: Stress distribution of the actual and predicted values.

## 4.2 Detachment Prediction

After training the multiple models multiple times and fine-tuning the hyperparameters, the following results were obtained.

1. In the 1<sup>st</sup> epoch, the training loss and validation losses are approximately 1.178 and 0.83 respectively. By the end of the 80<sup>th</sup> epoch the loss is saturated to approximately - 0.012 in training and 0.013 in validation sets.
2. Steady gradient descent can be observed in Figure 4.3. During saturation, the validation and training loss have approximately the same loss. This means that the model is not overfitted.
3. By the end of the training, the loss function is as low as 0.0098. Accuracy came out to 94.8 percent.
4. The test set got a loss of 0.018 which is very close to the training loss and validation loss. The test accuracy came out to 96.2 percent. Thus, the model is well fitted and does not suffer from overfitting and underfitting problems.
5. Therefore, without the need of performing the numerical simulations, the detachment mechanism of the curve can be found by feeding the interface curve to the deep learning model. The prediction has a test accuracy of 96.2 percent.

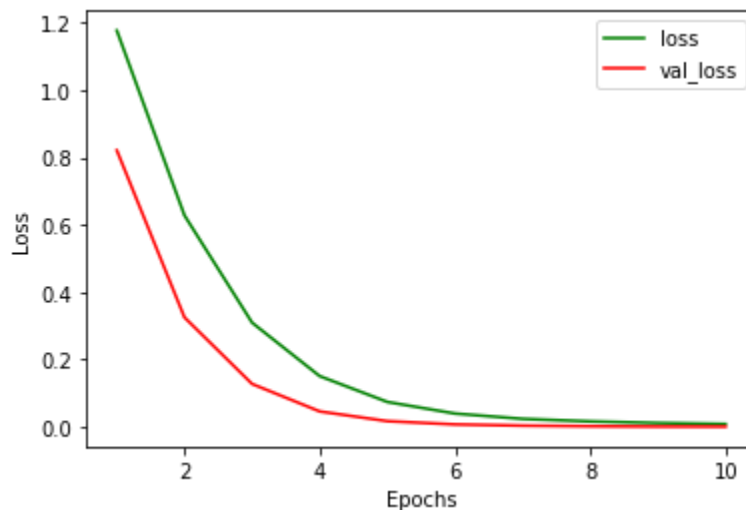


Figure 4.3: Loss vs Epochs(x 10 ) of the deep neural network for detachment prediction.

## 5. References:

- [1][https://www.researchgate.net/publication/257811043\\_Recent\\_advances\\_in\\_gecko\\_adhesion\\_and\\_friction\\_mechanisms\\_and\\_development\\_of\\_gecko-inspired\\_dry\\_adhesive\\_surfaces](https://www.researchgate.net/publication/257811043_Recent_advances_in_gecko_adhesion_and_friction_mechanisms_and_development_of_gecko-inspired_dry_adhesive_surfaces)
- [2] <https://arxiv.org/pdf/2102.11324>
- [3] <https://www.nature.com/articles/35015073>
- [4] <https://www.sciencedirect.com/science/article/pii/S0020768316000809>
- [5] <https://www.nature.com/articles/s41598-021-87383-9>
- [6] <https://www.sciencedirect.com/science/article/pii/S0022509616306548>
- [7][https://www.researchgate.net/figure/Structural-hierarchy-of-the-gecko-adhesive-system-A-Ventral-view-of-a-tokay-gecko\\_fig1\\_330047732](https://www.researchgate.net/figure/Structural-hierarchy-of-the-gecko-adhesive-system-A-Ventral-view-of-a-tokay-gecko_fig1_330047732)
- [8] <https://phys.org/news/2013-08-beetles-rubber-boots-scientists-ladybirds.html>